Electronic Supplementary Material (ESI) for RSC Advances

A Spring-Connected Nanogenerator Based on ZnO Nanoparticles and Multiwall Carbon Nanotube

—Supporting Information

Yi Yang[1,2,†], *He Tian*[1, 2,†], *Hui Sun*[1,2], *Run-Jie Xu*[1,2], *Yi Shu*[1,2], *Tian-Ling Ren*[1,2,*]

[1]Institute of Microelectronics, Tsinghua University, Beijing 100084, China

[2]Tsinghua National Laboratory for Information Science and Technology (TNList), Tsinghua University, Beijing 100084, China

†These authors contributed equally to this work

*Corresponding Author E-mail: RenTL@tsinghua.edu.cn

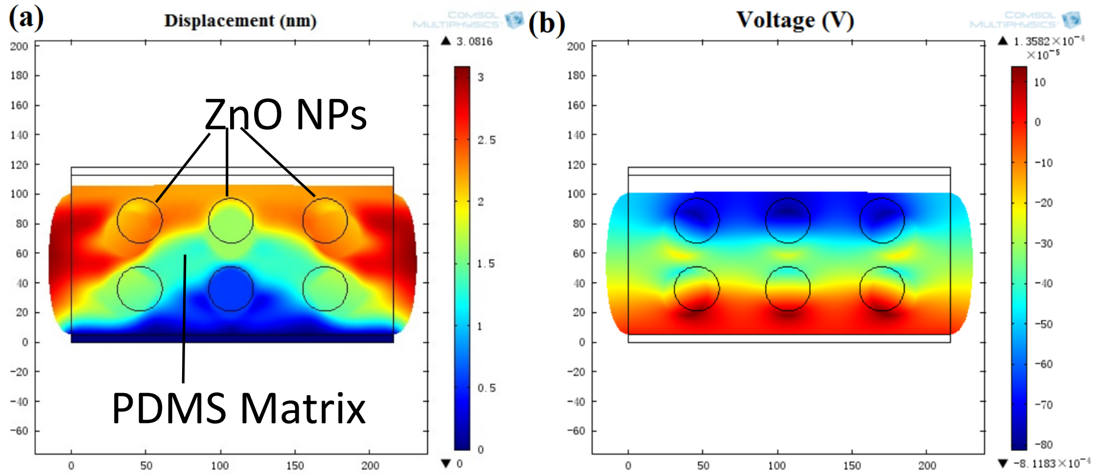

Figure S1. Finite Element Analysis (FEA) results of simplified model (a) the displacement of NG under 5N extrusion force which exhibits 3.0816 nm displacement (b) the output voltage of NG under 5N extrusion force which exhibits 0.13582 mV voltage on the top electrode

In order to simulate the performance of this device in theory, a simplified model of the NG is set up by COMSOL Multiphysics software. In this model, a slight layer with the thickness of 140 nm is extracted from the functional layer due to the extreme complexity of the whole device. Corresponding results are shown in Fig.S1 in which the round circles represent ZnO NPs scattering in the PDMS matrix as well as MW-CNT. It should be noted that the size and parameters are the same as the real situation and MW-CNT is embodied by relating parameters of matrix, instead of actual model setup. Fig.S1 (a) indicates that when being pressed by 5N extrusion force, this model displays 3.0816 nm displacement. While Fig.S1 (b) indicates that the output voltage is as high as 0.13582 mV under 5N extrusion force. It can be assumed that the whole functional layer is formed by such slight layers through parallel connection and the output voltage should be the sum of these output voltage elements. Consequently, the output voltage of a single functional layer could be as high as 9.7V in theory.

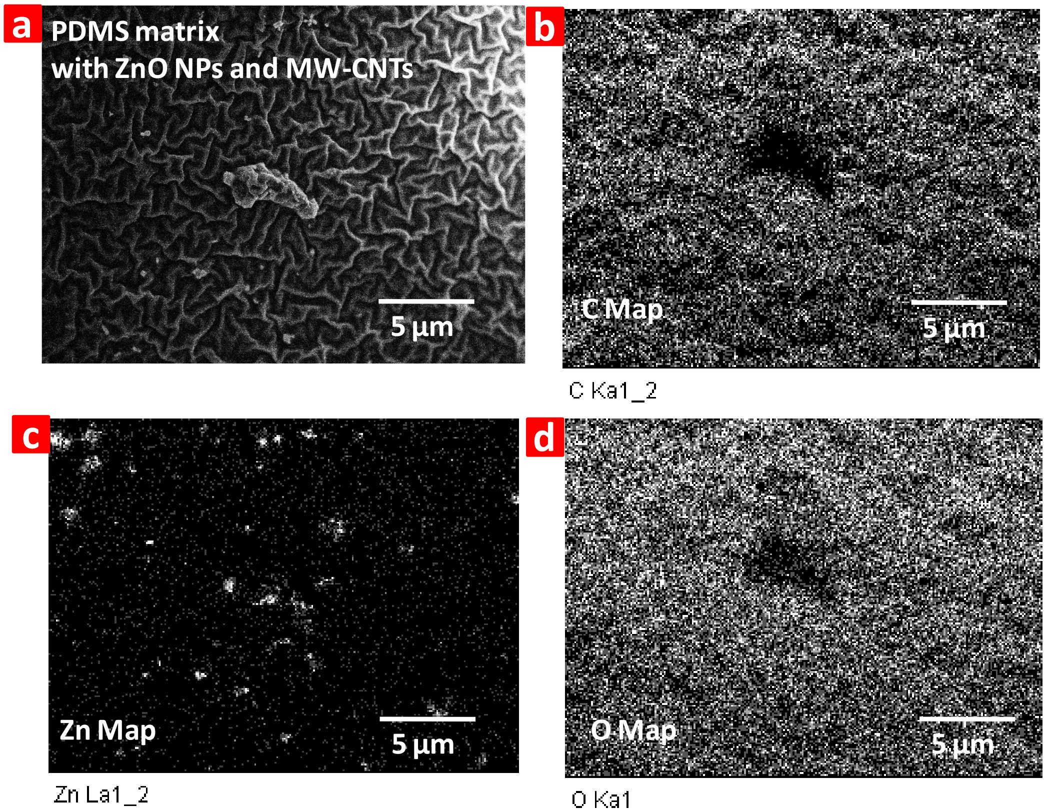

Figure S2. SEM image (a) and the corresponding elemental mapping for carbon (b), zinc (c) and oxygen reveal a homogeneous ZnO NPs and MW-CNT mixing in the PDMS.

Figure S2 shows the corresponding elemental mapping for carbon, zinc and oxygen, revealing a homogeneous mixing of ZnO NPs and MW-CNT in the PDMS.

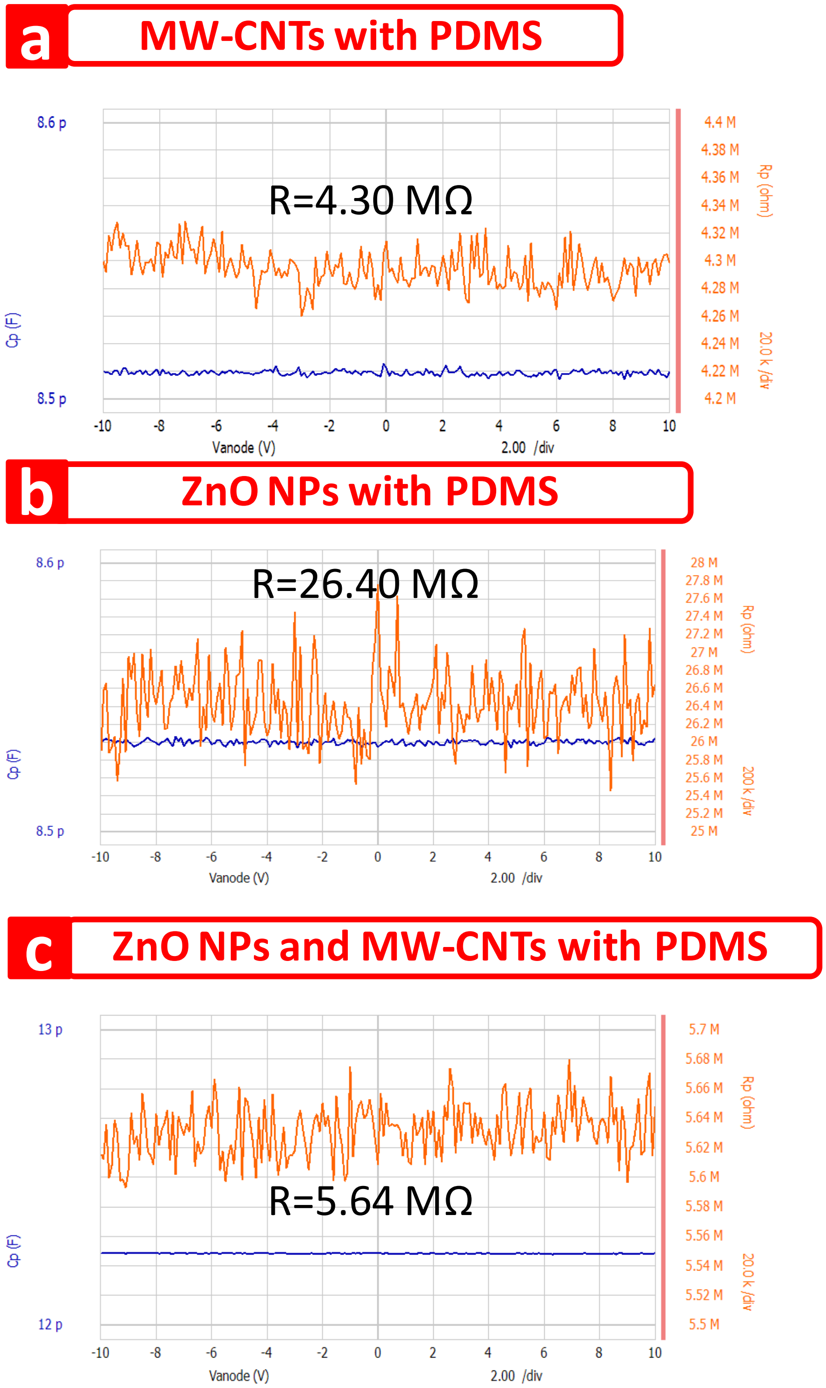

Figure S3. The comparison results of the resistance among MW-CNT with PDMS structure, ZnO NPs with PDMS structure and ZnO NPs and MW-CNT with PDMS structure under 100 k frequency using C-V Model.

Figure S3 displays the resistances of MW-CNT with PDMS structure, ZnO NPs with

PDMS structure and ZnO NPs and MW-CNT with PDMS structure successively under 100kHz frequency according to the C-V model. As shown in Figure S3, the resistance of MW-CNTs with PDMS structure is just 4.3 MΩ and the resistance of ZnO NPs with PDMS structure hits to 26.40 MΩ. For ZnO NPs and MW-CNT with PDMS structure, the resistance is 5.64 MΩ, which is just in between of previous two situations. These results prove the function of MW-CNT which efficiently enhances the conductivity of the whole device.

To obtain higher voltage theoretically, we establish finite element model and use Comsol multi-physics to figure it out. Figure S4a shows the Finite element model (FEM) results of the voltage distribution under condition of PDMS matrix with low conductivity. It is indicated that the ZnO NPs is almost isolated in the PDMS due to the low conductivity. Figure S4b shows that the FEM results of the voltage distribution under condition of PDMS matrix with high conductivity. It is indicated that the ZnO NPs is almost connected with each other in the PDMS due to the high conductivity. The relative conductivity vs. output voltage (Figure S4c) shows that the higher conductive film could produce higher voltage and the output voltage could saturated with further increasing conductivity. Since MW-CNT could enhance the conductivity of PDMS, this could enable the enhancement of output voltage.

Moreover, since MW-CNT could hold the NPs on its surface, this could make the ZnO NPs more uniform in PDMS. To demonstrate such idea, we also perform theoretical analysis. Figure S5a shows the FEM results of the voltage distribution under condition of ZnO NPs non-uniform distribution in PDMS. Figure S5b shows the FEM results of the voltage distribution under condition of ZnO NPs uniform distribution in PDMS. Compared with non-uniform ZnO NPs, relative conductivity vs. output voltage (Figure S5c) shows the uniform conductive film could produce higher voltage.

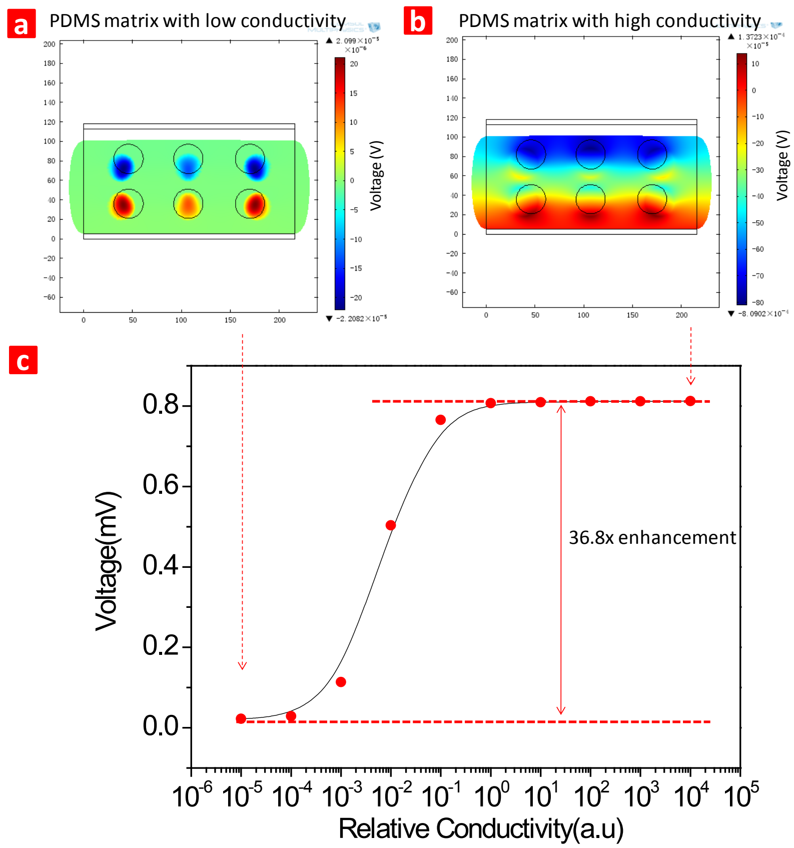

Figure S4. (a) Finite element model (FEM) results showing the voltage distribution under condition of PDMS matrix with low conductivity. It is indicated that the ZnO NPs is almost isolated in the PDMS due to the low conductivity. (b) FEM results showing the voltage distribution under condition of PDMS matrix with high conductivity. It is indicated that the ZnO NPs is almost connected with each other in the PDMS due to the high conductivity. (c) Relative conductivity vs. output voltage showing the higher conductive film could produce higher voltage and the output voltage could saturated with further increasing conductivity. Since MW-CNT could enhance the conductivity of PDMS, this could enable the enhancement of output voltage as high as 36.8 times.

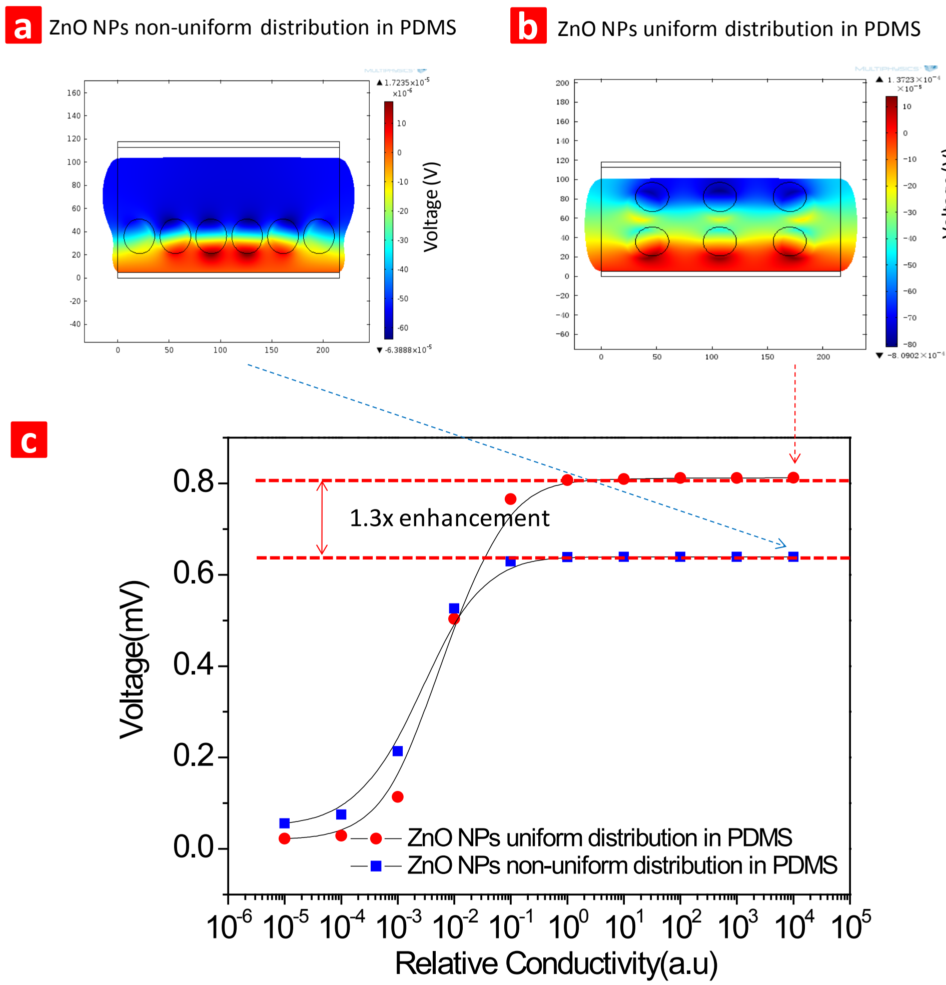

Figure S5. (a) Finite element model (FEM) results showing the voltage distribution under condition of ZnO NPs non-uniform distribution in PDMS. (b) FEM results showing the voltage distribution under condition of ZnO NPs uniform distribution in PDMS. (c) Compared with non-uniform ZnO Nps, relative conductivity vs. output voltage showing the uniform conductive film could produce higher voltage. Since MW-CNT could hold the NPs on its surface, this could make the ZnO NPs more uniform in PDMS.

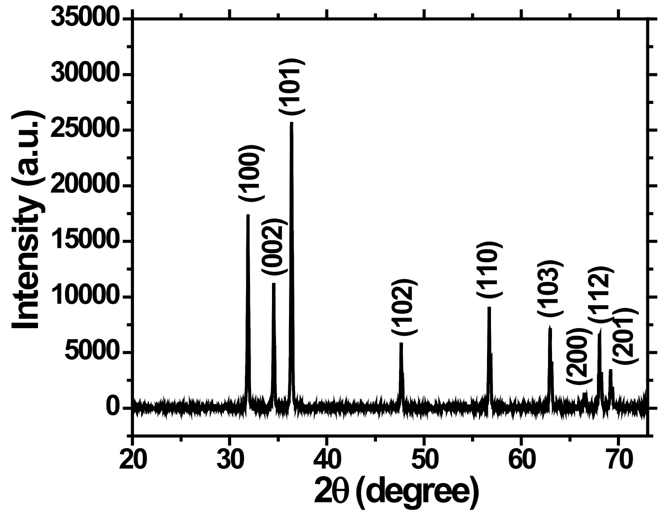

Figure S6. XRD pattern of ZnO NPs.

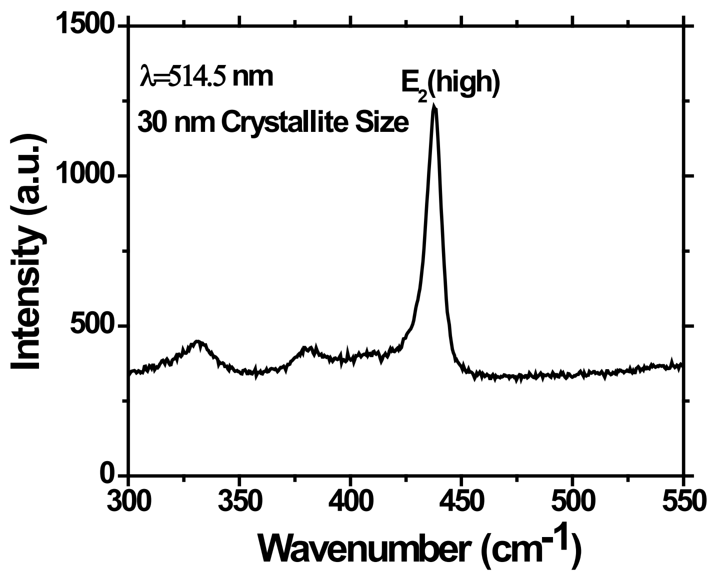

Figure S7. Raman spectra of ZnO NPs.

The material information of ZnO NPs is shown in Table S1. Figure S6 exhibit the X-ray diffraction (XRD) patterns of ZnO NPs, to characterize its crystalline structures. ZnO NPs show strong peaks at <100>, <002> and <101>. Unlike the images from SEM, X-ray diffraction (XRD) patterns shown in Figure S6 reveals the crystal structure of ZnO NPs. ZnO utilized here has polycrystalline structure. With the help of professional analysis software Jade and Scherrer formula, we have obtained the grain diameter for every crystal orientation of ZnO which is illustrated in Table S2. It is found that the grain diameter is far less than the diameter of particles shown in SEM image, thus we can infer that every particle is consist of multiple grains with various crystal orientations and may possibly leads to the output voltage and current under the non-specific direction of top and bottom electrodes.

Table S1 | The material information of ZnO NPs

Purity	99.9 %
Diameter	30 nm
Specific Surface Area	50 m^2/g
Color	milky white
Morphology	nearly spherical
Bulk density	0.3 - 0.45 g/cm^3
True density	5.606 g/cm^3

Table S2 | Grain diameter for every crystal orientation of ZnO

Crystal orientation	Grain diameter (nm)
(100)	2.8045
(002)	2.5949
(101)	2.4687
(102)	1.9070
(110)	1.6222
(103)	1.4751
(200)	1.4053
(112)	1.3766
(201)	1.3567

Figure S7 demonstrate the Raman spectrum obtained from ZnO NPs. The Raman spectrum of the ZnO NPs displays a E2-band at 437.7 cm^{-1}. Through fitting this peak, the crystallite size of ZnO NPs is estimated 30 nm, which is consistent with the Table S1 information provided from DK404, Beijing DK nano technology Co., LTD.

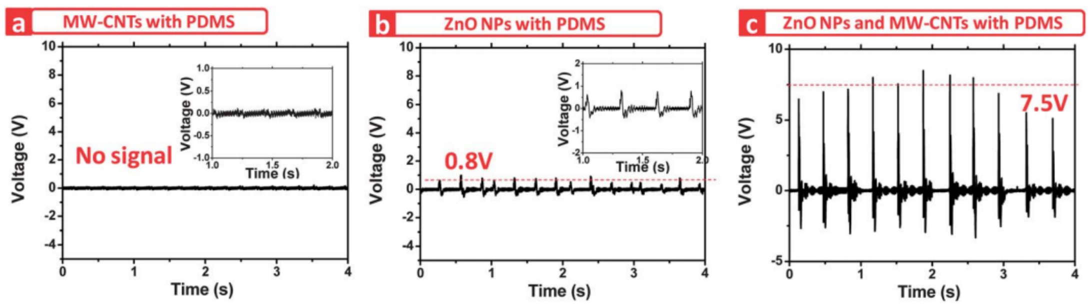

Figure S8. Comparison results among MW-CNT with a PDMS structure, ZnO NPs with a PDMS structure and ZnO NPs and MW-CNT with a PDMS structure. (a) Output voltages generated from the device MW-CNT with a PDMS structure. Inset shows the zoom in data. (b) Output voltages generated from the device ZnO NPs with a PDMS structure. Inset shows the zoom in data. (c) Output voltages generated from the device ZnO NPs and MW-CNT with a PDMS structure.